ISTITUTO NAZIONALE DI FISICA NUCLEARE - ISTITUTO NAZIONALE DI FISICA NUCLEARE - ISTITUTO NAZIONALE DI

Laboratori Nazionali di Frascati

LNF-90/001(P)
8 Gennaio 1990

E. De Sanctis, M. Anghinolfi, N. Bianchi, P. Corvisiero, S. Frullani, F. Garibaldi, G. Gervino, C. Guaraldo, P. Levi Sandri, V. Lucherini, V. Muccifora, E. Polli, A.R. Reolon, G. Ricco, P. Rossi, M. Sanzone, M. Taiuti, G.M. Urciuoli, A. Zucchiatti:

NUCLEAR PHYSICS AT FRASCATI WITH INTERNAL TARGETS

Invited talk at the
"Terzo Convegno su Problemi di Fisica Nucleare Teorica"
Cortona (October 16 - 18, 1989)
Presented by E. De Sanctis

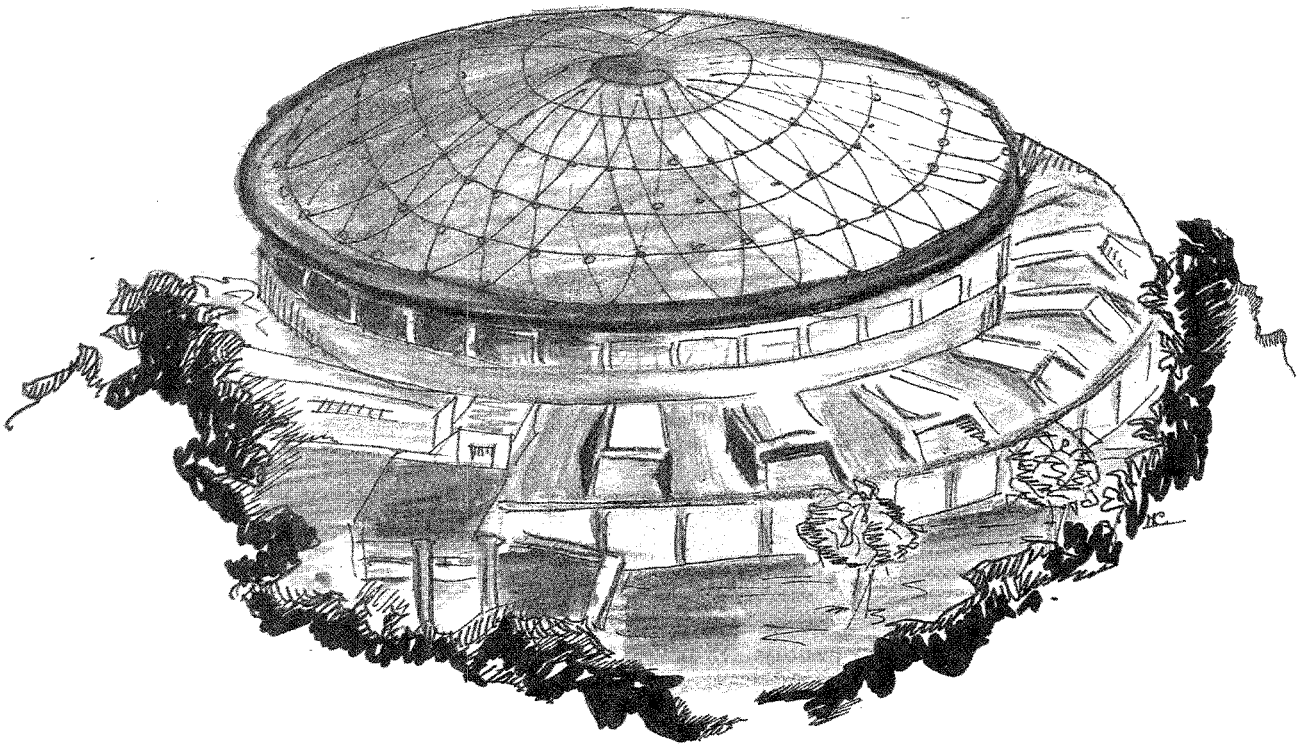

Servizio Documentazione
dei Laboratori Nazionali di Frascati
P.O. Box, 13 - 00044 Frascati (Italy)

ISTITUTO NAZIONALE DI FISICA NUCLEARE - ISTITUTO NAZIONALE DI FISICA NUCLEARE - ISTITUTO NAZIONALE DI FISICA NUCLEARE - ISTITUTO NAZIONALE DI

INFN - Laboratori Nazionali di Frascati
Servizio Documentazione

LNF-90/001(P)
8 Gennaio 1990

NUCLEAR PHYSICS AT FRASCATI WITH INTERNAL TARGETS

E. De Sanctis,[0] M. Anghinolfi,[1] N. Bianchi,[0] P. Corvisiero,[1] S. Frullani,[2] F. Garibaldi,[2] G. Gervino,[3] C. Guaraldo,[0] P. Levi Sandri,[0] V. Lucherini,[0] V. Muccifora,[0] E. Polli,[0] A.R. Reolon,[0] G. Ricco,[1] P. Rossi,[0] M. Sanzone,[1] M. Taiuti,[1] G.M. Urciuoli,[2] A. Zucchiatti[1]

[0] INFN-Laboratori Nazionali di Frascati, C.P. 13, I-00044 Frascati
[1] Dipartimento di Fisica dell'Università e INFN-Sezione di Genova, Via Dodecaneso 33, I-16146 Genova
[2] Laboratori di Fisica dell'Istituto Superiore di Sanità e INFN-Sezione Sanità, Viale Regina Margherita 229, I-00185 Roma
[3] Dipartimento di Fisica Sperimentale dell'Università e INFN-Sezione di Torino, Via P. Giuria 1, I-10125 Torino

ABSTRACT

The Argon condensed molecular beam installed at Frascati on the ADONE storage ring is described. The target is used to produce a tagged photon beam, of energy variable in the range 200-1200 MeV and intensity 10^6 photons/s per energy channel. The possibilities, advantages, and limitations of electron scattering experiments on internal-target are surveyed. Luminosities per nucleus of $\approx 10^{33} Z^{-2}$ cm^{-2} s^{-1} for electrons up to 1.5 GeV are achievable with 20 min. lifetime and good emittance for 100 mA circulating current and about 10^{13} atoms/cm^2 target thickness.

1. INTRODUCTION

The use of internal targets in storage and stretcher rings has been widely discussed[1-3] as a method of achieving reasonable high luminosity under conditions of low background, good energy resolution, negligible multiple scattering with minimal demands for beam from the primary accelerator. In its simplest realization the internal target configuration consists of a thin gaseous target of thickness in the range of 1-10 ng/cm^2 located to intercept the beam at a point in the lattice of a conventional stretcher or storage ring where the circulating particles are highly focoused. The high luminosity is achieved by recirculating the same particles through the target many times per second. The stored energy in the circulating beam is small compared to that dissipated in burying an external beam of comparable luminosity. Consequently, backgrounds and shielding requirements for an internal target facility are modest compared to those for a conventional external beam installation.

Concerning the electromagnetic reaction, this approach represents an attractive option for performing in a cheap way some of the experiments foreseen in the coming continuos beam high duty cycle accelerators. After few pioneering experiments using internal gas targets at Novosibirsk[4] in the past decade, a proposal has been recently presented to use this technique on the PEP storage ring,[5] and three rings are under construction at Novosibirsk,[6] Bates[7] and NIKHEF[8] for allowing a systematic exploitation of such experiments.

Foreseeing this great interest in nuclear physics studies with electromagnetic probes, in 1985 a collaboration between Frascati Laboratory and Genova University[9-10] started a program to install an Argon clustered molecular beam on the electron storage ring ADONE for studying the interaction of circulating electrons with the Argon jet, and producing a monochromatic high energy photon beam through the tagging technique.

In this paper we describe briefly the ADONE internal target facility (Section 2) and the Argon condensed target (Section 3), and give the preliminary results on the characteristics of the tagged photon beam (Section 4), and a fast survey of the experimental program (Section 5).

2. THE EXPERIMENTAL FACILITY

Fig. 1(a) shows a schematic layout of the positron-electron storage ring, ADONE: the ring is divided into 12 identical regions each consisting of a lattice elements (a n=1/2 bending magnet with a quadrupole doublet on each side) and a 2.6 m long straight insertions for experiments. The circumference of the ADONE ring is approximately 105 m, so that a bunch of ultrarelativistic electrons takes about T_0=350 ns to make a round. Electrons are injected into the storage ring at an energy of ≈340 MeV (a few-turn injection will result in about 70 mA current circulating in the ring) and then accelerated to the desired energy by rising the magnetic field of the guiding magnets

(this operation requires about 20 s). The 51.4 MHz RF-cavity groups the circulating electrons into 18 bunches, each ≈1 ns wide and ≈20 ns apart.[11]

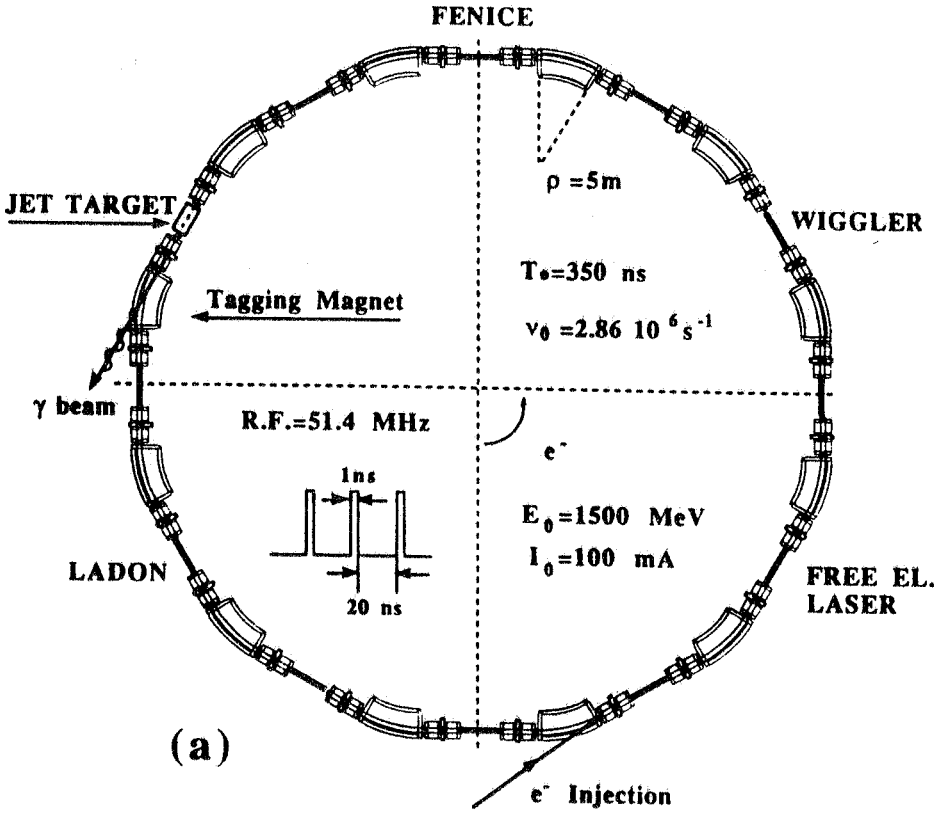

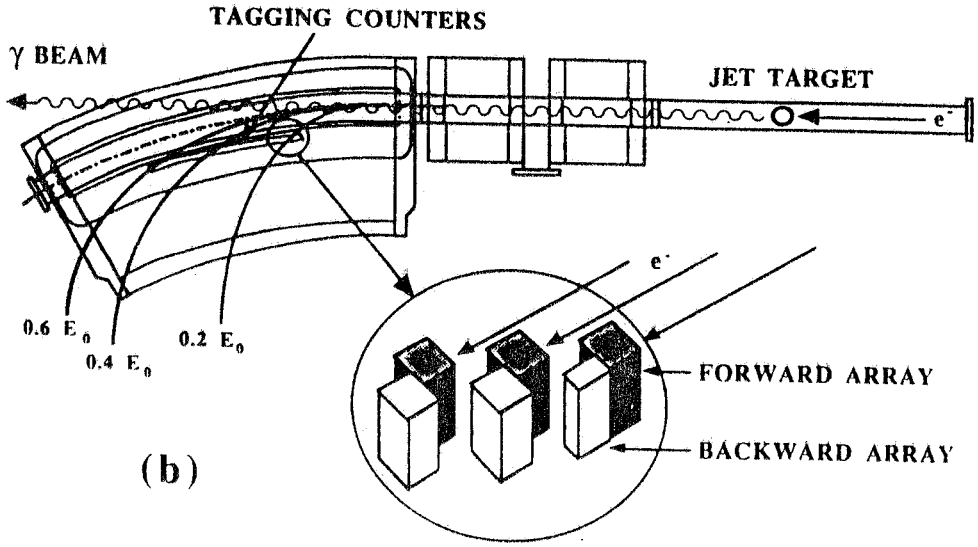

Fig.1 (a) An overview of the ADONE storage ring showing the Argon jet target location; and, Fig. (b), of the tagging spectrometer and counters.

The photon tagging technique, long used to monochromate bremsstrahlung, is essentially a method for identifying individuals photons of a given energy ($k\pm\Delta k$) from a continuous bremsstrahlung spectrum. This is achieved by measuring the residual energy E of the original electron of energy E_0 in the electron beam incident on the bremsstrahlung radiator, after it has emitted a "monochromatic" photon of energy $k=E_0-E$. This is performed by measuring in coincidence the residual electron and the product x of the photoreaction: then, from the experimental point of view, the tagging technique can be considered as an electron scattering coincidence experiment -(e,e'x) experiment-, where the exchanged photon is real.[10]

The jet target (which acts as a radiator) is placed in the straight section n° 5 between consecutive lattice elements; the recoil electrons are momentum analyzed by the next dipole magnet and detected by two arrays of scintillation counters in coincidence (39 counters in each array), placed between the ring vacuum pipe and the dipole magnet flux return joke [Fig. 1 (b)].The scintillators define 76 energy channels, and have different sizes to give the same photon energy resolution (≈1% at E_0=1500 MeV and ≈2.7 % at E_0=500 MeV) over the whole tagging range $k=(0.4\text{-}0.8)E_0$ (E_0 being the energy of the machine).

3. THE ARGON CONDENSED TARGET

The used target is a condensed molecular beam[12] which provides a flow of gas at supersonic speed (hence the name of gas jet target) due to the expansion of gas from a vessel at high pressure into the vacuum through an injector of very small aperture and special geometry. Argon atoms condensate into microclusters of 10^5-10^6 atoms which minimize the transverse momentum of the atoms and thus the opening angle of the jet. Skimmers further suppress the tail of the density profiles relative to the core.

A side view of the Argon jet target is shown in Fig. 2. As it is seen, the target consists of three parts: i) the jet injection system (the cone installed above the ring) where the jet is produced with the help of a special trumpet-shaped nozzle and several collimating orifices; ii) the interaction chamber, where the molecular jet crosses the electron beam at about 25 cm from its source point; iii) the jet dump (the cone installed below the ring), which has to ensure that the jet is pumped away without significant backstreaming.

Three differential pumping stages have been interposed to separate both the jet-injection and the jet-dump chambers from the vacuum pipe in order to minimize the pressure rise in the interaction region. Each room between two successive orifices is pumped on by a 360 l/s turbomolecular pump, which is directly flanged to the relevant vacuum chamber, while both the expansion and sink chambers are evacuated by a high speed (1000 l/s) turbomolecular pump. Two fast acting UHV valves separate the production and sink chambers from the ADONE vacuum pipe to easy the jet on/off operations and to prevent the possible contamination of the ring in case

of a large pressure bump due to breakdown of the target system.

The operation of the target are controlled by a microprocessor-based system which performs all tasks to start up the jet on/off procedure, recording of the measurements, and safety checks.

The operating conditions are: inlet pressure and temperature 1÷20 bar and about 300 °K, respectively; nozzle throat diameter 87 μm and semiaperture 3.5°. From a total flux of $\approx 10^{20}$ Ar-atoms/s expanding from the nozzle, the collimator system selects about 10^{17}-10^{18} atoms/s, which corresponds to a target thickness of 1÷10 ng/cm^2 (∅=6 mm) on the path of the electron beam (that is at a distance of ≈25 cm from the nozzle).

The measured density ρ (and thickness) of the Argon jet at the interaction point as a function of the inlet pressure are shown in Fig. 3. ρ is given by the expression:

$$\rho = \frac{m\Phi}{Sv}$$

where m is the molecular mass (in g),S and v are the molecular jet cross sectional area and velocity at the interaction point, Φ is the clustered jet flux, given by the product ($v_s \cdot P_s$) of the evacuating pumping speed and the pressure in the sinking chamber.

As shown in the figure, the transition from gaseous to clustered jet occurs for inlet pressure of about 5.5 bar, and produces a sudden increase on the jet density.

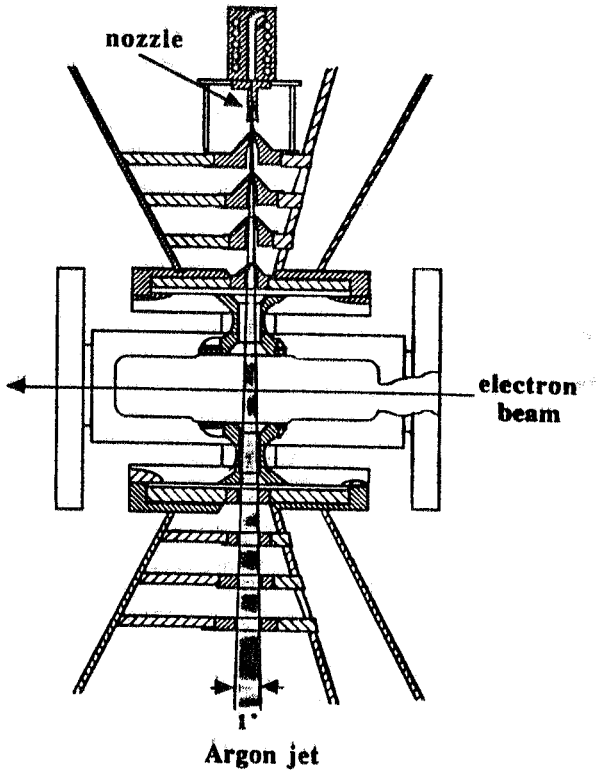

Fig.2 Cut away view of the central section of the Argon jet target: the direction of the cluster jet and ADONE electron beam are indicated.

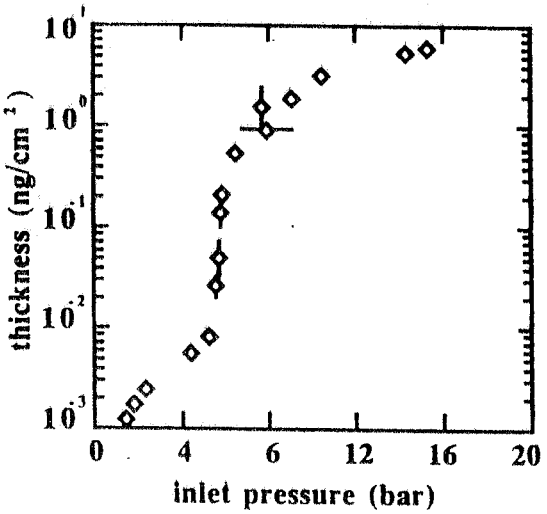

Fig. 3 Argon-Jet thickness versus inlet pressure.

Fig 4 shows the jet profiles measured by moving the electron beam radially, while keeping its trajectory parallel to the straight section axis, and recording the rate of the tagging counters, which is proportional to the product of the overlap between the Argon jet and the electron beam. The solid lines are the results of the convolutions of the electron beam size (gaussian with σ=1.5 mm at 1500 MeV) with a cylindric jet of radius equal to 6 mm.

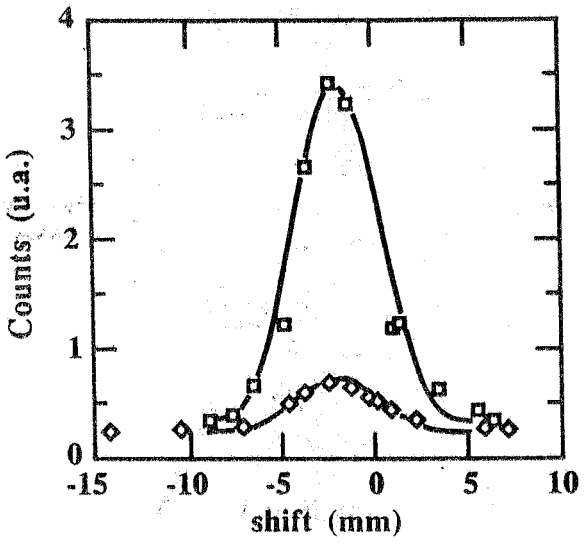

The measurements of the jet profile were repeated several times at different initial electron energies and jet thickness: the results obtained were in an excellent agreement among each other.

Fig.4 Measured Argon jet profiles at the electron beam intersection point for two jet thickness (o, 0.3 ng/cm^3 and ◊, 0.03 ng/cm^3, respectively).

4. PRELIMINARY RESULTS

After the injection of electrons in the ring and the rise in energy up to the required value, the Argon jet is fired across the ADONE vacuum pipe: this fact cuts down the electron beam lifetime to the value $T_0/(\sigma_\varepsilon \rho)$, being T_0 the revolution period, σ_ε the removal cross section, and ρ the jet thickness. Then the cycle is ended by lowering again the field of the magnets to the injection value.

The Argon jet thickness is so small that, at energies higher than 450 MeV, neither the Coulomb scattering nor ionization losses contribute to the beam quality degradation, being the RF-cavity able to compensate for both the growth in divergency and the mean energy losses.[13] As for the beam lifetime, the removal cross section involves only those processes of bremsstrahlung in which the electrons lose sufficient energy to place them outside the acceptance band-width ε of the ring (ε=0.01E_0). This is easily seen in Fig. 5, where the beam lifetime values measured for a few jet thickness are compared with the result of a calculation performed using the above described relation (solid line curve).

In order to measure the tagging efficiency and probability, a BGO crystal spectrometer will be used. The spectrometer consists of four cylindrical BGO crystals, each 9.5 cm in diameter and 8 cm long, aligned one behind the other so as to offer a total thickness of 29 radiation lengths to the photon beam. Each BGO crystal is coupled to six photomultipliers to improve light collection. As an example, Fig. 6 shows the bremsstrahlung spectra produced by 1200 MeV electrons on a 0.01 ng/cm^2 Argon jet as registered by this spectrometer in single (a) and in coincidence with one

tagging channel (b): the ≈2.7 % peak resolution is in good agreement with the calculations: the contribution of residual gas in the straight section (≈ 6 m long) is responsible for this high resolution value.

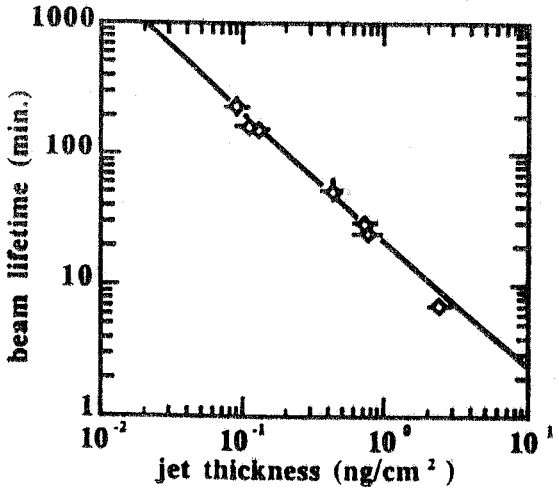

Fig. 5 ADONE electron beam lifetime versus the Argon jet thickness. The solid line is the curve $t=T_0/(\sigma_\varepsilon\rho)$

The intensity of the photon beam in the tagging range is given by[9,10]

$$N_\gamma = N_0 \rho v_0 \sigma_{br}(k_1 k_2 E_0)$$

where N_0 is the average number of circulating electrons, ρ the jet thickness, v_0 the number of recirculations per second, and

$$\sigma_{br}(k_1 k_2 E_0) = \frac{1}{X_0}\left[\frac{4}{3} ln \frac{k_2}{k_1} - \frac{4}{3}\frac{k_2 - k_1}{E_0} + \frac{k_2^2 - k_1^2}{2 E_0^2}\right]$$

is the bremsstrahlung cross section (times the ratio N/A between the Avogadro and the mass numbers) integrated between k_1 and k_2, and X_0 the Argon radiation length.

When $k_1=0.4\cdot E_0$, $k_2=0.8\cdot E_0$, the average circulating current ≈60 mA, and ρ= 5 ng/cm^2, we obtain $N_\gamma = 6\cdot 10^7$ photons/s, that is about $7.5\cdot 10^5$ photons/s per energy channel.

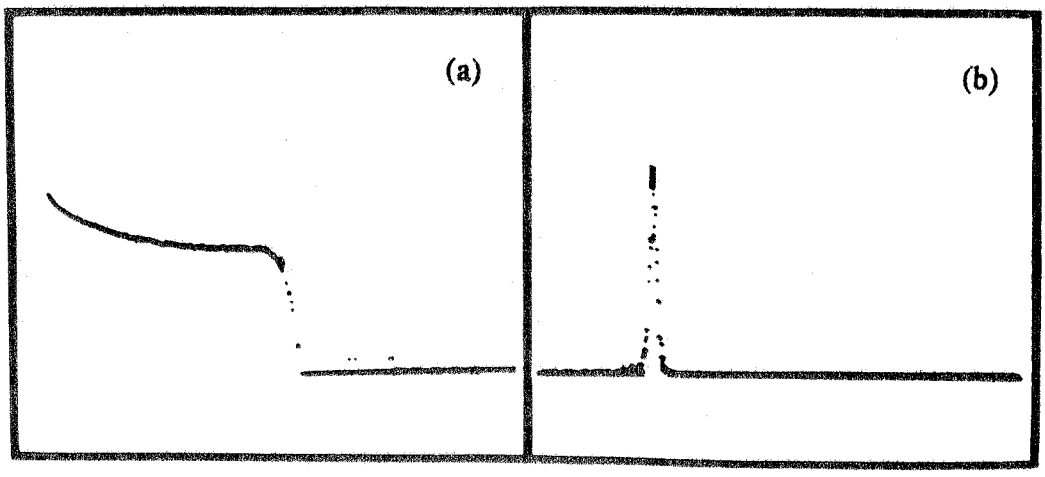

Fig. 6 Bremsstrahlung spectra produced by 1200 MeV electrons on a 0.01 ng/cm^2 Argon jet: BGO answers in single (a), and in coincidence with one tagging channel (b), respectively.

Since the determination of the photon energy relies on a coincidence between the tagging counters and the detector for the photoejected particles, the tagging method is subjected to usual

limitation due to random coincidences between the tagging and the reaction product detectors.[10,14] Then, the usable photon flux is proportional to the duty factor of the electron beam and inversely proportional to the experimental time resolution of the coincidence, τ_r. Because of the time structure of the circulating beam (18 bunches, each about τ_0=1 ns wide and about 20 ns apart, which cross the clustered jet $2.86 \cdot 10^6$ times per second), and since $\tau_0 < \tau_r$, the true-to-accidentals ratio R is proportional to the crossing frequency.[14] Therefore, in the actual operating mode and for a ratio R =1, the maximum photon flux is about $6 \cdot 10^5$ γ/s per energy channel. The installation of a new 350 MHz RF-cavity in the spring 1991 will groups the circulating electrons into 123 bunches 2.86 ns apart, and allow an increase by a factor $\approx$7 of the photon intensity for the same ratio R (or of R for the same photon intensity).

THE EXPERIMENTAL PROGRAM

1. Photoreactions

The first experiment planned is the measurement of the total absorption nuclear cross section between 500 MeV and 1200 MeV.[15] In this energy region there are available only the measurements on light and medium heavy nuclei (Be, C, Al, H_2O and Cu) made at Erevan with a tagged bremsstrahlung photons.[16] Unfortunately, those data, which where collected with a large acceptance over the initial photon energy, fluctuate well above the experimental errors. When one takes their mean values, normalized to the atomic number A, two facts emerge[17] (see Fig.7), specifically: i) the disappearance of nucleonic resonances, at about 700 and 1000 MeV, clearly evident in the photoabsorption on proton and deuteron; and ii) the onset of the shadowing effect at about 1100 MeV.

This result, which would validate the Weise[18] hypothesis that some shadowing effects in nuclei should manifest below 2 GeV, has been contradicted by the claim of absence of shadowing effects below 3.2 GeV, deduced by the same authors[19] from more recent data on electrofission of ^{238}U at low Q^2. Clearly, it is necessary to produce new reliable data.

For light nuclei, the transmission technique will be used,[15] monitoring the photon flux with and without the absorbing target on the beam: the total photonuclear cross section is then deducible by subtracting the large atomic contribution, which for light nuclei is calculable with good accuracy.[20] The experimental apparatus has been installed: tagged photons cross a 60 cm long graphite absorber put inside a 1.2 Tesla magnetic field and are detected, about 13 m downstream, by the above described BGO spectrometer. This geometry affords good rejection of the forward components of the electromagnetic showers created in the absorber.

For heavy nuclei, the Uranium isotopes photofission will be studied, being the fission cross section equal the total inelastic cross section. The highly-ionizing fission fragments will be detected by using Parallel Plate Avalanche Detectors.[21]

The excitation of an isobaric resonance in a nucleon bound in the nucleus is however subject to propagation and rescattering effects which may lead to collective or partially collective behaviour.

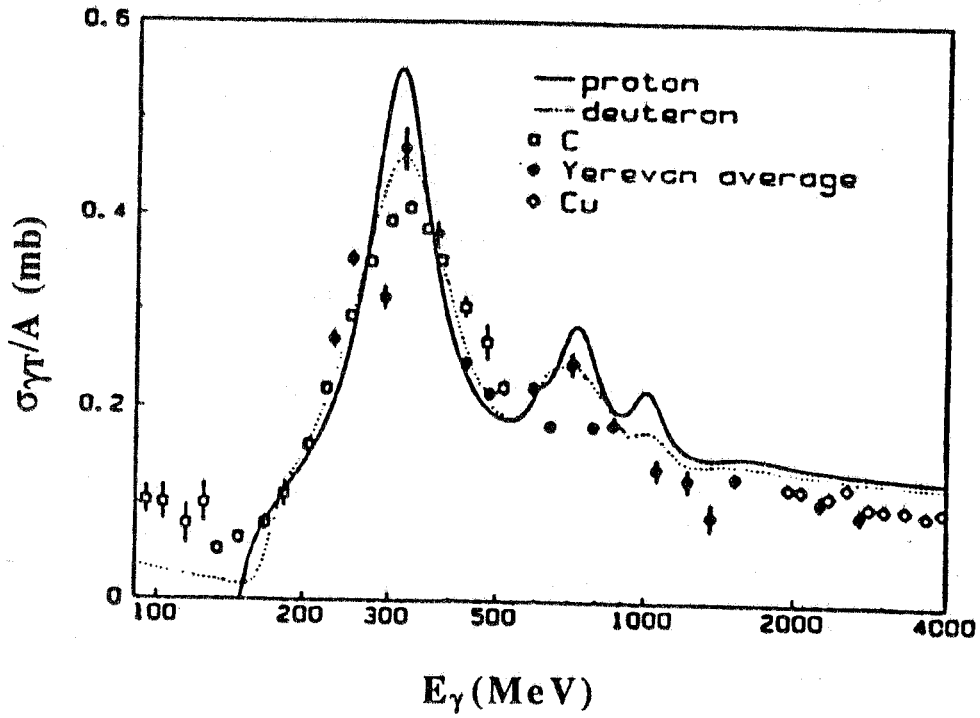

Fig.7 Behaviour of the total photonuclear cross section per nucleon versus photon energy (reprinted from Ref.15).

In this respect there are many open questions: the correlations among nucleons may produce collective phenomena like the propagation of the isobars and the excitation of collective nuclear resonances. Here the question is whether these effects can still be described in terms of isobars only, or it is more convenient to turn to quark degrees of freedom. In fact, the nuclear medium seems to favour the quark deconfinement and the formation of multiquark clusters, such as dibaryons, which in addition can also be strongly deformed and coloured. The spreading width may therefore originate from the overlap of a larger number of nuclear states of rather complex nature which can be identified and separated only by accurate spectroscopy of the various decay channels.[22]

Since all the observed resonances decay mainly in the πN channel, the photoproduction of pions on nuclei should be very useful for the investigation of the high energy excitation mechanism in the nuclei. This is particularly true if also the emission of one nucleon in coincidence with the produced pion is measured. Many high energy photoreactions can be suggested for the study of these aspects. A particular role is played by exclusive processes with two hadrons in the final state detected in coincidence.A partial list of experiments include: i) (γ,NN), for the analysis of correlation effects and short range phenomena, ii) (γ,πN), for the study of excited structure due to both the modifications induced by the nuclear medium on the single baryon states and to the

production of nuclear resonances; ii) $(\gamma,\pi\pi)$ for the observation of meson resonances in nuclei and of the photon hadronization generated by vector meson production.

In order to compensate for the low cross section of several interesting experiments a large solid angle detector (a BGO crystal ball of about 3.6π srd) is under construction for the detection of neutral photoejected particles.[23] It consists of 480 BGO crystals, each 24 cm long (21 radiation lengths), grouped into 15 sectors in ϑ plane (angular acceptance from 25° to 155°) by 32 in the φ plane. The crystals are arranged as a rugby ball in order to present constant absorption length over the whole covered solid angle. A bore of 20 cm diameter along the major axis of the ball will allow the passage of the beam.The mechanical support, presently under construction, is a modular system in carbon fibers organized as a main iron frame supporting 24 baskets each housing 20 crystals.

Other experiments presently under consideration for this beam are:

- the measurement of the differential cross section for the photodisintegration of a deuteron exclusively into a proton and neutron for photon energies between 500 and 1200 MeV. This will allow to verify whether above 1000 MeV the cross section at large momentum transfer behaves according to the simple constituent-counting rule, as suggested by the Napolitano et al.[24] data at 90°, and study the behaviour of the forward-to-backward ratio of the differential cross section in order to check the prediction of a simple quark model.[25]

- photon scattering from the proton in the Δ excitation region, to study the nucleon-excitation configuration.[26] At energies above the pion threshold only few experimental data exist mainly because of the difficulty of the experiment, arising from the competing process of π^0 photoproduction decaying into photons and thus leading to photon-nucleus final states.

b) Electroreactions

Thin targets inside a storage ring can be used to carry out electron scattering experiments. The requirement that targets be thin enough to prevent loss of superior beam quality and allow a sufficiently long beam lifetime generally leads to low luminosities. (The luminosity is a measure of the event rate for a given cross section, given by the product of beam current and target thickness). The argument may be particularly critical for the electromagnetic interactions for which cross sections are of the order of 10^{-33} cm^2sr^{-1} per nucleon around 1 GeV.

As above said, in the ADONE case the removal cross section involves only those processes of bremsstrahlung in which the electrons lose sufficient energy to place them outside the acceptance band-width of the ring. Consequently, for any target the beam loss would be proportional to $\rho \cdot Z^2$, where ρ is the target density in nuclei/cm^2 and Z is the atomic number of the target. In Fig. 8 are shown the limiting density and luminosity as functions of A available at ADONE for a 20 minutes storage lifetime, and for 100 mA stored current. As it is seen, the maximum luminosity per nucleus is about $10^{33}Z^{-2}$ $cm^{-2}s^{-1}$.

Although the external target luminosities are in general $\geq 10^{35}$ $cm^{-2}s^{-1}$, such internal target luminosities are more than sufficient to carry out an interesting program of electromagnetic studies, particularly when using large solid angle detectors. In any case, the advantage of the internal target method as opposed to an external target with an extracted beam is evident in experiments involving the detection of low energy highly ionizing particles such as recoiling target nuclei, deuteron and alfa particles, or fission products, where energy loss in the target is of prime importance. In fact, in this case the high circulating current permits the use of a very thin target to give luminosity higher than for an external target with a low current.

Moreover, there is another important parameter to consider for this comparison, specifically the trues-to-accidentals ratio, which, besides the coincidence and singles rates, is determined by the coincidence resolving time τ_r, and the beam structure. From this point of view, storage rings are similar to continuous beam machine. As an example, ADONE, with the new 350 MHz RF, will provide a bunch of $1.7 \cdot 10^9$ electrons every 2.86 ns, that is a number of electrons per bunch several order of magnitude lower than for the conventional external beams, and a repetition rate close to 10^9 Hz, which is the usual value for a C.W. machine.

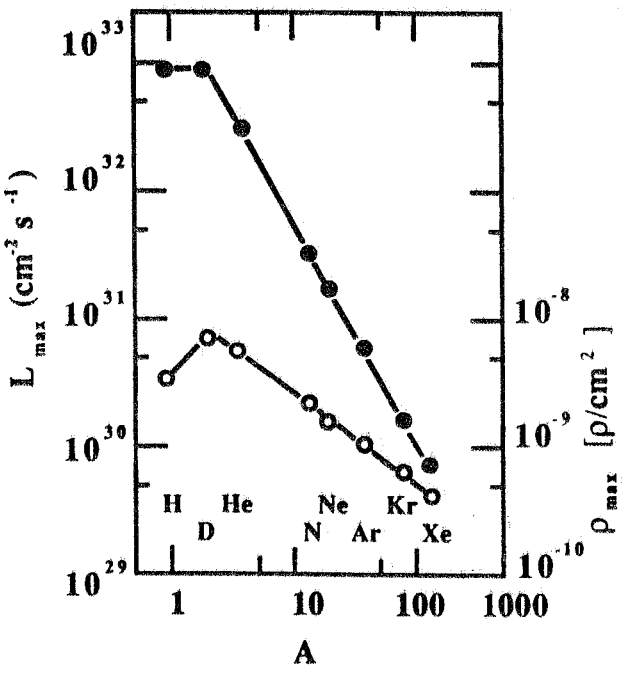

Fig.8 Calculated maximum luminosity for a 20 minutes beam lifetime (upper curve and left ordinate scale) and the target density (lower curve and right ordinate scale) as a function of the atomic weight A.

Two electron scattering experiments are presently under consideration, specifically:

i) the quasi elastic inclusive scattering on ^{16}O from 500 up to 1500 MeV, with separation of the longitudinal and transverse components of the cross section.[27] The scattered electrons will be simultaneously detected at two angles by two spectrometers, each consisting of a front position sensitive detector (scintillating optical fibers), and of an energy loss and energy detector (NaI crystals, and a 20-crystal cluster of the BGO ball); and

ii) the elastic electron scattering on deuteron to measure the deuteron electromagnetic form factor for momentum transfers up to $Q^2 \approx 2.2$ $(GeV/c)^2$ by detection of deuterons scattered at 15°.

This experiment will allow to verify the results of the recent measurement at SLAC by R.G. Arnold et al.,[28] who have found a $B(Q^2)$ behaviour in qualitative agreement with impulse

approximation calculations.The expected counting rates evaluated for a luminosity of $\approx 10^{33}$ $cm^{-2}s^{-1}$ and a solid angle of ≈ 1 sr are equal to those used in the SLAC experiment.[28]

References

1) Proc. Workshop on the Use of Electron Ring for Nuclear Physics, Lund, October 5-7, 1982, Ed.J.O. Adler and B. Schroder.
2) Proc. Workshop on Electronuclear Physics with Internal Targets, SLAC, January 5-8,1987, Eds. R.G. Arnold and R.C. Minehart SLAC-316,UC-34C and January 9-12, 1989, in print.
3) Proc. Workshop on Internal Targets Physics with Electron beam , Amsterdam Sep. 6, 1989, NIKHEF-K Internal Report, in print.
4) L.S. Korobeinikov, L.M. Kurdadze, A.P.Onuchin, S.G. Popov, and G.M. Tumaikin, Sov. J. Phys. 6, 61 (1968), and G.I. Budker, A.P.Onuchin, S.G. Popov, and G.M. Tumaikin, Sov. J. Phys., 6, 563 (1968).
5) K. Van Bibber et al., PEGASYS: a Proposal for an Internal Target Spectrometer Facility at the PEP Storage Ring, unpublished.
6) V.F. Dmitriev et al., Phys. Lett. 157B, 143 (1985), and Nucl. Phys. A464, 237 (1987).
7) MIT-Bates Upgrade Proposal, MIT June 1984.
8) T.S. Bauer, H.P. Blok, C.W. De Jager, P.K.A. De Witt Huberts, NIKHEF Internal Report, WR-529 (1988).
9) M. Albicocco et al., Frascati Internal Report, LNF 86/29 (R), (1986).
10) V. Muccifora and E. De Sanctis, Frascati Internal Report, LNF 86/30 (R), (1986).
11) F. Tazzioli , ADONE Internal Memorandum, T-121, Dec. 16, 1985..
12) M. Taiuti et al., Proc.Topical Conf on Electronuclear Physics with Internal Targets, SLAC, January 9-12,1989, in print.
13) V. Muccifora et al., Frascati Internal Report, (1990), in press.
14) R.J. Griffiths et al., Nucl. Instr. and Meth.,40,181(1966).
15) M. Anghinolfi et al. Frascati Internal Report, LNF 89/045 (R) (1989).
16) E. A. Arakelyan et al., Sov. J. Nucl. Phys. 38,589 (1983).
17) R. Bergère, Proc.2nd Workshop on Perspectives in Nuclear Physics at Int. Energies, Trieste, March 25-29, 1985, p.153, Eds. S. Boffi, C. Ciofi degli Atti and M.M. Giannini, World Scientific,Singapore 1985.
18) W.Weise, Phys. Rep. 2, 53 (1974).
19) E. A. Arakelyan et al., Erevan preprint YERPHI-1103 (66)-88)
20) J. H. Hubbell et al., Phys. Chem. Ref. Data, 9,01023 (1980).
21) P. Garganne, Saclay Internal Report, CEA-N-2492 (1986).

22) M.M. Giannini, Proc. of the Workshop on Heavy-Quark Factory and Nuclear Physics Facility with Superconducting Linacs, Courmayeur,14-17 Dec. 1987. Eds. E. De Sanctis, M. Greco, M. Piccolo, and S. Tazzari, p.907.

23) A. Zucchiatti, Proc. of the Workshop on Heavy-Quark Factory and Nuclear Physics Facility with Superconducting Linacs, Courmayeur,14-17 Dec. 1987. Eds. E. De Sanctis, M. Greco, M. Piccolo, and S. Tazzari, p. 965.

24) J.Napolitano et al., Phys. Rev. Lett. 61, 2530 (1989).

25) E. De Sanctis, A.B. Kaidalov and L.A. Kondratyuk, Frascati Internal Report, LNF 89/087 (1987), submitted to Phys. Rev. C.

26) M. Sanzone et al. FOMAMI Proposal-INFN Gruppo III (1987)., and Proc. Int. School of Intermediate Energy Nuclear Physics Verona 1981, Eds R. Bergère, S. Costa, and C. Schaerf, World Scientific, Singapore 1982, p. 291.

27) M. Anghinolfi et al., ESCAF Proposal-INFN Gruppo III (1989).

28) R.G. Arnold et al., Phys. Rev. Lett., 58,1723 (1987).